

PAPER • OPEN ACCESS

Fidelity-optimized quantum state estimation

To cite this article: Amir Kalev and Itay Hen 2015 *New J. Phys.* **17** 093008

View the [article online](#) for updates and enhancements.

You may also like

- [Computable entanglement conversion witness that is better than the negativity](#)
Mark W Girard and Gilad Gour
- [High-frequency approximation for periodically driven quantum systems from a Floquet-space perspective](#)
André Eckardt and Egidijus Anisimovas
- [Multipoles and vortex multiplets in multidimensional media with inhomogeneous defocusing nonlinearity](#)
Rodislav Drében, Nir Dror, Boris A Malomed et al.

New Journal of Physics

The open access journal at the forefront of physics

Deutsche Physikalische Gesellschaft 

IOP Institute of Physics

Published in partnership
with: Deutsche Physikalische
Gesellschaft and the Institute
of Physics



OPEN ACCESS

RECEIVED
19 June 2015

ACCEPTED FOR PUBLICATION
3 August 2015

PUBLISHED
9 September 2015

Content from this work
may be used under the
terms of the [Creative
Commons Attribution 3.0
licence](#).

Any further distribution of
this work must maintain
attribution to the
author(s) and the title of
the work, journal citation
and DOI.



PAPER

Fidelity-optimized quantum state estimation

Amir Kalev¹ and Itay Hen^{2,3}

¹ Center for Quantum Information and Control, University of New Mexico, Albuquerque, NM 87131-0001, USA

² Information Sciences Institute, University of Southern California, Marina del Rey, CA 90292, USA

³ Center for Quantum Information Science & Technology, University of Southern California, Los Angeles, CA 90089, USA

E-mail: amirk@unm.edu

Keywords: quantum state estimation, self-correcting, optimization protocol

Abstract

We describe an optimized, self-correcting procedure for the Bayesian inference of pure quantum states. By analyzing the history of measurement outcomes at each step, the procedure returns the most likely pure state, as well as the optimal basis for the measurement that is to follow. The latter is chosen to maximize, on average, the fidelity of the most likely state after the measurement. We also consider a practical variant of this protocol, where the available measurement bases are restricted to certain limited sets of bases. We demonstrate the success of our method by considering in detail the single-qubit and two-qubit cases, and comparing the performance of our method against other existing methods.

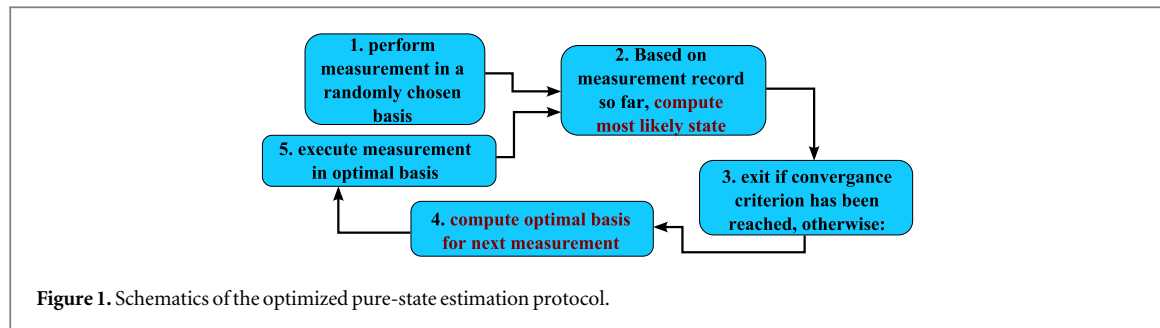
1. Introduction

Quantum technology is a fast developing area of both experimental and theoretical research. It has well-known applications in computation protocols [1–6] and communication protocols [7–12], as well as in the study of fundamental physical phenomena [13–16]. A particular interest in advanced technology is that of devising protocols for basic primitives which are meant to serve as building blocks for other, more involved applications. One example of this is quantum state estimation (QSE), whose purpose is to estimate the state of a quantum system based on a measurement record of a finite ensemble of identical systems.

It is a common practice in QSE (and in many other protocols) to have the quantum device complete a program which is then followed by a classical processing step during which conclusions are drawn. However, with advanced technologies and the growing control over quantum devices, comes the obvious need (and possibility) to integrate these two steps into one indivisible unit within which the program and the data-processing steps are repeated successively—feed-backing each other to form one efficient, self-correcting, self-executing quantum protocol. Indeed, there has been a growing interest in devising and implementing *in situ* protocols [17–27], in particular using a Bayesian statistical inference, with various degrees of automation where the measurement at later steps depends on the information acquired in previous steps. Some of these ideas were successfully implemented using current technology [23] and were shown to improve accuracy quadratically over common protocols.

In any adaptive QSE protocol, the sequence of measurements depends on a choice of a figure of merit. For example, Huszár and Houslsby [21] considered an adaptive protocol using a Bayesian learning strategy derived from maximization of the average information gain. While such a strategy guarantees that each measurement yields, on average, the maximal information gain, it is not clear how it performs in terms of average infidelity (or equivalently, fidelity). Infidelity is a particularly important figure of merit in QSE as it quantifies the QSE inaccuracy (see, e.g., [23] and references therein).

With the goal of minimizing estimation inaccuracy in mind, this paper discusses a QSE protocol based on Bayesian statistical inference whose objective is the maximization of the average fidelity. The physical setup that we consider is one in which an ‘oven’ prepares and emits copies of an unknown quantum pure state of a given dimension d . We are then given the task of providing an estimation with the highest average fidelity to the state of the system by performing orthogonal projective (von Neumann) single-copy measurements.



The heart of the protocol consists of two subroutines: (1) the computation of the most likely candidate for the state emitted by the oven, and (2) based on the fidelity as a figure of merit, a computation of an optimal basis for the next measurement. The resultant proposed protocol is therefore an optimized, fully automated, self-correcting algorithm.

In the following, we describe the protocol as it applies to systems of finite-dimensional Hilbert spaces. We then study its performance by considering different situations and practical examples in order to elucidate the rather intuitive guiding principles of the protocol. In particular, we examine a ‘real-world’ variant of the protocol, where the experiment is limited to measurements in certain restricted settings. We conclude with a summary and suggestions for possible follow-up research directions.

2. The protocol

The main idea behind the protocol suggested here is the analysis, after each measurement, of the entire history of measurement outcomes thus far. The analysis yields the most likely state emitted by the oven and a basis for the next measurement. The latter is chosen such that measurement outcomes lead to new estimations whose average fidelity to the emitted state is maximal. Based on this analysis, a measurement is then performed in the calculated basis and the routine is repeated. By optimizing the measurement to be performed such that it will yield, at each step, the highest average fidelity, the proposed protocol maintains minimal inaccuracy in state estimation throughout its course.

We now define the steps of the protocol in detail. We assume, for simplicity, that no prior information concerning the distribution over which the oven is emitting the pure states is provided (the modifications required to address the more general case will be discussed below). The reader is referred to figure 1 for a schematic diagram of the protocol.

- Step 1: at first, no information about the state emitted by the oven has been acquired. The program thus executes a measurement in a randomly chosen basis, and records the result.
- Step 2: based on all recorded outcomes so far, the program computes the (pure) state most likely to have yielded the sequence of measurement outcomes. The details of this computation are given below. We denote the most likely state after k measurements by $|\Psi_k\rangle$.
- Step 3: if some predetermined stopping criterion has been reached, e.g., the fidelity $|\langle\Psi_{k-1}|\Psi_k\rangle|^2 < 1 - \epsilon$, for a required accuracy level ϵ , the program halts.
- Step 4: after finding the most likely state, the program computes the optimal basis for the measurement that is to follow. The optimality condition is derived and discussed below. In practice, the experiment may be limited to a subset of measurement bases. We will also discuss the required adjustments to the protocol in the presence of such limitations.
- Step 5: the program executes a measurement in the calculated basis, records the outcome, and returns to step 2.

2.1. Calculating the most likely pure state

We now address the details of computing the pure state that represents our knowledge about the emitted state after k iterations of the above protocol have taken place (and k measurements have been executed).

Let us consider the k th iteration of the protocol. At each iteration, one measurement is performed on a single copy of the emitted state. Let $S_k = \{|\phi_1\rangle, |\phi_2\rangle, \dots, |\phi_k\rangle\}$ be the sequence of the k measurement outcomes obtained and recorded thus far. Based on the sequence S_k , we are interested in finding the pure state that has the

maximum fidelity with the emitted state. However, since we do not know what the emitted state is, we must average over all possible states, weighing each according to its probability of having been emitted (based on all recorded outcomes thus far). The *most likely pure state of the system* $|\Psi_k\rangle$ would then be the pure state that has the maximal fidelity, on average, with all possible emitted states, namely:

$$|\Psi_k\rangle = \operatorname{argmax}_{\tilde{\psi}} \int dP(\psi | \mathcal{S}_k) |\langle \tilde{\psi} | \psi \rangle|^2. \quad (1)$$

Here, $dP(\psi | \mathcal{S}_k)$ is the (infinitesimal posterior) probability that the oven emitted a state $|\psi\rangle$ given the sequence of measurement outcomes obtained so far.

Interestingly, the above expression can be rewritten as

$$|\Psi_k\rangle = \operatorname{argmax}_{\tilde{\psi}} \langle \tilde{\psi} | \rho_k | \tilde{\psi} \rangle, \quad (2)$$

where ρ_k is the state which best represents the totality of our knowledge so far about the system, given \mathcal{S}_k ,

$$\rho_k = \int dP(\psi | \mathcal{S}_k) |\psi\rangle\langle\psi|. \quad (3)$$

Therefore, $|\Psi_k\rangle$ is the pure state with the highest fidelity to ρ_k , i.e., it is the state corresponding to the largest eigenvalue of ρ_k ,

$$|\Psi_k\rangle = \operatorname{argmax}_{\tilde{\psi}} \langle \tilde{\psi} | \rho_k | \tilde{\psi} \rangle = |\lambda_{\rho_k}^{\max}\rangle. \quad (4)$$

To evaluate $dP(\psi | \mathcal{S}_k)$, we apply Bayes' formula $dP(\psi | \mathcal{S}_k) = P(\mathcal{S}_k | \psi) dP(\psi) / P(\mathcal{S}_k)$, where $P(\mathcal{S}_k | \psi)$ is the probability of obtaining the outcome sequence \mathcal{S}_k provided that the emitted state is $|\psi\rangle$, and is given through Born's rule $P(\mathcal{S}_k | \psi) = \prod_{m=1}^k |\langle \phi_m | \psi \rangle|^2$.

The probability function $dP(\psi)$ reflects our knowledge about the distribution over which the oven is choosing the states to emit, $dP(\psi) = p(\psi) d\psi$, where $p(\psi)$ is the corresponding probability density, and $d\psi$ is a Haar-measure over the pure-state manifold. Consequently, the probability of obtaining the sequence of measurement outcomes is $P(\mathcal{S}_k) = \int d\psi P(\mathcal{S}_k | \psi) p(\psi)$. Combining the above, we arrive at:

$$dP(\psi | \mathcal{S}_k) = \frac{d\psi p(\psi) \prod_{m=1}^k |\langle \phi_m | \psi \rangle|^2}{\int d\psi p(\psi) \prod_{m=1}^k |\langle \phi_m | \psi \rangle|^2}. \quad (5)$$

Now, since we are assuming that no prior information about the distribution over which the oven is emitting the states is given, we can set $p(\psi) = \text{constant}$ ⁴, which in turn allows us to identify the conditional (or posterior) infinitesimal probability $dP(\psi | \mathcal{S}_k)$ as

$$dP(\psi | \mathcal{S}_k) = \frac{d\mathcal{P}_k}{\int d\mathcal{P}_k}, \quad (6)$$

where we have defined:

$$d\mathcal{P}_k = d\psi \prod_{m=1}^k |\langle \phi_m | \psi \rangle|^2. \quad (7)$$

With the above definitions, we can rewrite the state that represents our knowledge about the system, equation (3), in the following way

$$\rho_k = \frac{\int d\mathcal{P}_k |\psi\rangle\langle\psi|}{\int d\mathcal{P}_k} = \frac{\int d\psi \prod_{m=1}^k |\langle \phi_m | \psi \rangle|^2 |\psi\rangle\langle\psi|}{\int d\psi \prod_{m=1}^k |\langle \phi_m | \psi \rangle|^2}. \quad (8)$$

The above calculation can be generalized to include the case where some *a priori* knowledge about the distribution over which the oven emits the states is given, in which case $p(\psi)$ would no longer be constant. This may be of interest—for example, when one wishes to certify that a particular target state has been experimentally realized. Additionally, the calculation of ρ_k may be used to establish a stopping criterion for the protocol, e.g., by setting a threshold for the purity of the state, namely, $\text{Tr}[\rho_k^2] > 1 - \epsilon$ for a small predetermined ϵ .

2.2. Optimizing the basis of measurement

Next, we describe a procedure to optimize the basis of the measurement to follow. The next measurement basis is calculated based on all the previous measurement outcomes. It is chosen to maximize the fidelity between our

⁴ The constant equals $\frac{\pi^{d-1}}{(d-1)!}$ [28].

knowledge about the emitted state and the most likely state, as it would be computed after the measurement has been performed.

Let \mathcal{S}_{k-1} be the set of the $k - 1$ measurement outcomes obtained and recorded, and let $\tilde{\mathcal{B}}_k = \{|\tilde{e}_{k,1}\rangle, |\tilde{e}_{k,2}\rangle, \dots, |\tilde{e}_{k,d}\rangle\}$ be the orthonormal basis states of the k th measurement over which the optimization would be carried out. Suppose now that a measurement has taken place in the $\tilde{\mathcal{B}}_k$ basis with the outcome $|\tilde{e}_{k,n}\rangle$ (for some $1 \leq n \leq d$). The fidelity between the most likely state and our knowledge about the state of the system would be

$$\lambda_{\rho_{k,n}}^{\max} = \max_{\tilde{\psi}} \left| \tilde{\psi} \right| \left[\frac{\int d\mathcal{P}_{k,n} |\psi\rangle \langle \psi|}{\int d\mathcal{P}_{k,n}} \right] \left| \tilde{\psi} \right|, \quad (9)$$

with $\mathcal{P}_{k,n}$ as defined in equation (7) with $\mathcal{S}_{k,n} = \mathcal{S}_{k-1} \cup \{|\tilde{e}_{k,n}\rangle\}$.

However, since we do not know which of the measurement outcomes will be realized, in order to optimize the basis $\tilde{\mathcal{B}}_k$, we must consider all possible outcomes and weigh them according to their *a priori* probability of occurring. This results in a weight-averaged maximal fidelity, $\sum_{n=1}^d P(\tilde{e}_{k,n}|\mathcal{S}_{k-1}) \lambda_{\rho_{k,n}}^{\max}$, where $P(\tilde{e}_{k,n}|\mathcal{S}_{k-1})$ is the probability of obtaining the outcome $|\tilde{e}_{k,n}\rangle$ given our knowledge so far:

$$\begin{aligned} P\left(\tilde{e}_{k,n} \mid \mathcal{S}_{k-1}\right) &= \left| \langle \tilde{e}_{k,n} \mid \rho_{k-1} \mid \tilde{e}_{k,n} \rangle \right| \\ &= \frac{\int d\mathcal{P}_{k-1} \left| \langle \tilde{e}_{k,n} \mid \tilde{\psi} \rangle \right|^2}{\int d\mathcal{P}_{k-1}} = \frac{\int d\mathcal{P}_{k,n}}{\int d\mathcal{P}_{k-1}} \end{aligned} \quad (10)$$

We define the *optimal basis of measurement* as the one which maximizes this weight-averaged maximal fidelity. Combining the expression above with the expression for $\lambda_{\rho_{k,n}}^{\max}$ in equation (9), the optimal basis of measurement simplifies to

$$\mathcal{B}_k = \operatorname{argmax}_{\{|\tilde{e}_{k,1..d}\rangle\}} \sum_{n=1}^d \lambda_{\rho_{k,n}}^{\max}, \quad (11)$$

where $\varrho_{k,n}$ is the ‘unnormalized’ density matrix

$$\varrho_{k,n} = \int d\mathcal{P}_{k,n} |\psi\rangle \langle \psi|. \quad (12)$$

The optimal basis thus neatly reduces to the basis which maximizes the sum of the largest eigenvalues of $\varrho_{k,n}$ with $n = 1, 2, \dots, d$.

By weighing equally the contributions from each of the possible measurement outcomes, equation (11) offers some intuition as to the optimal choice for the next basis of measurement: that the probability to obtain any outcome, $\langle \tilde{e}_{k,n} \mid \rho_{k-1} \mid \tilde{e}_{k,n} \rangle$, is independent of the outcome label, i.e., $\langle \tilde{e}_{k,n} \mid \rho_{k-1} \mid \tilde{e}_{k,n} \rangle = 1/d$, suggests that at each measurement step one should probe the system, in parameter space, in directions where our ignorance about the outcome is maximal, that is, in a basis that is *unbiased* to ρ_{k-1} . In the next section we study several explicit examples illustrating the above intuitive interpretation of this infidelity-minimizing cost function.

3. Optimized pure qubit state estimation

As a case study, let us now consider the performance of the above protocol for the identification of a Haar-random pure qubit state. Since for a qubit the Hilbert space is isomorphic to the Bloch sphere, the maximization at each stage can be performed with respect to the two real variables corresponding to the polar angle θ and the azimuthal angle φ of the orientation of the Bloch vector of the qubit.

3.1. First few measurements

To gain some insight into the nature of the protocol, we examine in some detail its first few iterations as they apply to the qubit case. This will allow us to appreciate the intuitive interpretation of the protocol.

Prior to the first measurement, no information about the state of the system is given. Thus, according to the proposed protocol, the first measurement is performed in a randomly chosen basis which we shall denote as $\{| \uparrow \rangle, | \downarrow \rangle\}$. For simplicity, let us denote the outcome direction of that first measurement by $| \uparrow \rangle$. At this point, the most likely pure state of the system is simply $| \uparrow \rangle$. (Hereafter, we represent density matrices and states in the basis as $\{| \uparrow \rangle, | \downarrow \rangle\}$.) To determine the basis in which the next ($k = 2$) measurement will be performed, one should solve equation (11), given the measurement record $\mathcal{S}_1 = \{| \uparrow \rangle\}$. Upon doing so, the following set of degenerate solutions is found:

Table 1. First few measurements of the single-qubit state estimation protocol. The figures in the right-most column represent the posterior distribution given the measurement record. The color code red-to-blue indicates high-to-low probability regions. The black arrow represent the most likely state on the Bloch sphere, while the red arrows represent the fidelity-maximizing basis for the next measurement.

Measurement index k	(Unnormalized) most likely state $ \Psi_k\rangle$	Most likely state fidelity	Next basis of measurement $\{ e_k\rangle\}$	Measurement outcome	Bloch sphere representation
0	—	1/2	$\{ \uparrow\rangle, \downarrow\rangle\}$	$ \uparrow\rangle$	
1	$ \uparrow\rangle$	2/3	$\{ \rangle, -\rangle\}$	$ +\rangle$	
2	$(\uparrow\rangle + +\rangle)$	$\frac{1}{2} + \frac{\sqrt{2}}{6}$	$\{ \rangle + i\rangle, -\rangle - i\rangle\}$	$ +i\rangle$	
3	$(\uparrow\rangle + +\rangle + +\rangle + i\rangle)$	$\frac{1}{2} + \frac{\sqrt{3}}{6}$	unbiased to $ \Psi_3\rangle$		

$$\{ |e_2(\varphi)\rangle \} = \left\{ \frac{|\uparrow\rangle + e^{i\varphi}|\downarrow\rangle}{\sqrt{2}}, \frac{|\uparrow\rangle - e^{i\varphi}|\downarrow\rangle}{\sqrt{2}} \right\}. \quad (13)$$

Without loss of generality, we take $\varphi = 0$, so that the second measurement basis is

$$\{ |e_2\rangle \} = \left\{ |\pm\rangle = \frac{1}{\sqrt{2}}(|\uparrow\rangle \pm |\downarrow\rangle) \right\}. \quad (14)$$

Performing the second measurement, we can again assume, without loss of generality, that the result $|+\rangle$ had been obtained. The most likely pure state describing the system, up to normalization, is $|\Psi_2\rangle = (|\uparrow\rangle + |+\rangle)$, i.e., pointing in the direction $(\theta, \varphi) = (\pi/4, 0)$ on the Bloch sphere.

To determine the basis of the next measurement, $k = 3$, one should solve equation (11) given the outcome record $\mathcal{S}_2 = \{|\uparrow\rangle, |+\rangle\}$. In this case, we obtain the solution

$$\{ |e_3\rangle \} = \left\{ |\pm i\rangle = \frac{1}{\sqrt{2}}(|\uparrow\rangle \pm i|\downarrow\rangle) \right\}. \quad (15)$$

As discussed in the previous section, we find that the optimal measurement basis at each step so far is in a direction that is unbiased to the most likely state, namely $|\langle \Psi_{k-1} | e_{k,n} \rangle|^2 = 1/d = 1/2$.

At this point we can assume again that the third measurement result is $|+i\rangle$; this yields, for the most likely pure state describing the system, up to normalization, the state $|\Psi_3\rangle = (|\uparrow\rangle + |+\rangle + |+\rangle + i\rangle)$ —i.e., pointing in the direction $(\theta, \varphi) = (\arccos \frac{1}{\sqrt{3}}, \frac{\pi}{4})$ on the Bloch sphere.

So far, the optimal sequence of measurement bases has formed a set of mutually unbiased bases (MUBs). It follows then that the initial optimal probing sequence of the state naturally generates mutually orthogonal directions on the Bloch sphere. The fourth measurement basis is obtained by solving equation (11) given the measurement record $\mathcal{S}_3 = \{|\uparrow\rangle, |+\rangle, |+i\rangle\}$ which obviously cannot yield a fourth MUB. Nonetheless, the solution in this case is found to be degenerate, corresponding to all directions that are unbiased to $|e_{4,n}\rangle$, namely, $|\langle \Psi_3 | \psi \rangle|^2 = 1/2$ (equivalently, all vectors in a Bloch sphere orthogonal to the Bloch vector of $|\Psi_3\rangle$). A summary of the first few measurements is given in table 1.

3.2. Comparison with information-gain strategy

As another illustrative example, we compare the performance of the proposed protocol against the performance of another strategy in which information-gain is used as a figure of merit (the reader is referred to [21] for more details). Specifically, we analyze the first few steps of the two protocols for the case where the emitted qubit state is known *a priori* to lie in the $x - y$ plane of the Bloch sphere, i.e., that $p(\psi)$ is not a constant, but obeys $p(\psi) \sim \delta(\theta - \pi/2)$.

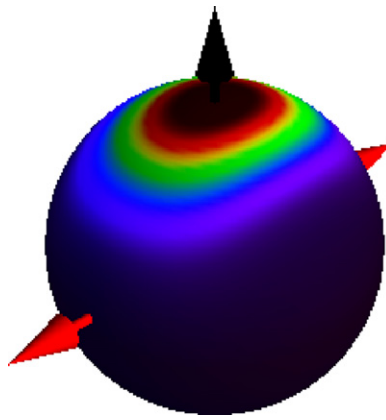


Figure 2. Measurement direction in the limit of many copies. The figure presents the most likely vector (black arrow) and the optimal measurement basis (red arrows) for the sequence of measurements of equation (16) with $k_1 = 6$, $k_2 = 3$ and $k_3 = 1$. The false color plot corresponds to the probability density of $dP(\psi|\mathcal{S}_k)$ for the above sequence of outcomes. The example illustrates that the optimal basis of measurement is mutually unbiased to the most likely state, and moreover, points in the ‘direction of least information’ (in this example, the y axis).

In the first step of the two protocols, no prior information about the direction of the qubit in the $x - y$ plane of the Bloch sphere is given. Therefore, without loss of generality, we assume that the first measurement is performed in the $\{|e_1\rangle\} = \{| \pm \rangle\}$ basis, and its outcome is $|+\rangle$. As for the second measurement basis, it is interesting that both protocols yield the same next-measurement basis—namely, $\{|e_2\rangle\} = \{| \pm i \rangle\}$. Assuming, without loss of generality, that the outcome here is $|+i\rangle$, i.e., that $\mathcal{S}_2 = \{|+\rangle, |+i\rangle\}$, we move on to calculate the next basis of measurement. Here again, in both protocols, regardless of whether we optimize with respect to information-gain or infidelity, the same measurement direction is obtained for the third measurement, namely, $\{|e_3\rangle\} = \{\frac{1}{\sqrt{2}}(|\uparrow\rangle \pm e^{\frac{3i\pi}{4}}|\downarrow\rangle)\}$, which unsurprisingly is found to be unbiased to the most likely state $|\Psi_2\rangle = \frac{1}{\sqrt{2}}(|\uparrow\rangle \pm e^{\frac{i\pi}{4}}|\downarrow\rangle)$.

It is in the fourth iteration, in which the next basis of measurement is computed based on the outcome record $\mathcal{S}_3 = \{|+\rangle, |+i\rangle, \frac{1}{\sqrt{2}}(|\uparrow\rangle + e^{\frac{3i\pi}{4}}|\downarrow\rangle)\}$, that the information-gain figure of merit [21] and the infidelity figure of merit begin yielding different measurement directions. Here, numerical methods must be employed, yielding the directions $\phi_{\text{max-fid.}} = 2.9113(2)$ and $\phi_{\text{inf-gain.}} = 2.9322(2)$ for the fidelity-maximizing and information-gain methods, respectively. Importantly, we note that in using the fidelity-optimized strategy, we ensure that the fourth measurement basis has a maximal average fidelity, illustrating that maximal information-gain does not necessarily correspond to minimal inaccuracy.

3.3. Asymptotic behavior

In the following, we consider the basis of measurement that follows the sequence of outcomes

$$\mathcal{S}_k = \left\{ \underbrace{|\uparrow\rangle, \dots, |\uparrow\rangle}_{k_1 \text{ times}}, \underbrace{|+\rangle, \dots, |+\rangle}_{k_2 \text{ times}}, \underbrace{|-\rangle, \dots, |-\rangle}_{k_2 \text{ times}}, \underbrace{|+i\rangle, \dots, |+i\rangle}_{k_3 \text{ times}}, \underbrace{|-i\rangle, \dots, |-i\rangle}_{k_3 \text{ times}} \right\}, \quad (16)$$

where $k = k_1 + 2k_2 + 2k_3$ is the total number of measurements. Although somewhat contrived, the above sequence provides the key ingredients to understanding the asymptotic behavior of the protocol, within the limit of a large number of copies. First, we note that for any value of $k_i > 0$, $i = 1, 2, 3$, the most likely state is $|\uparrow\rangle$. Employing the fidelity-optimizing protocol described above, it is easy to show that the optimal basis of the next measurement is $\{| \pm \rangle\}$ if $k_2 > k_3$ and $\{| \pm i \rangle\}$ if $k_2 < k_3$. (If $k_2 = k_3$, both axes are equally optimal.) That is, the measurement basis vectors point in the direction in which we are ‘most ignorant.’ This is illustrated in figure 2 which shows the color-coded probability measure $dP(\Psi|\mathcal{S}_k)$ along with the most likely vector (black arrow) and the next measurement basis (red arrows) in the case $k_1 = 6$, $k_2 = 3$ and $k_3 = 1$. This is in accord with the intuitive interpretation of equation (11) which was discussed previously.

In particular, the above holds true for large k , in which case the probability measure $dP(\psi|\mathcal{S}_k)$ is sharply peaked around the most likely state, i.e., around $|\uparrow\rangle$. In this case, the information-gain maximization approach [18, 21] dictates that the next measurement should be performed in a basis where one of its vectors points in a

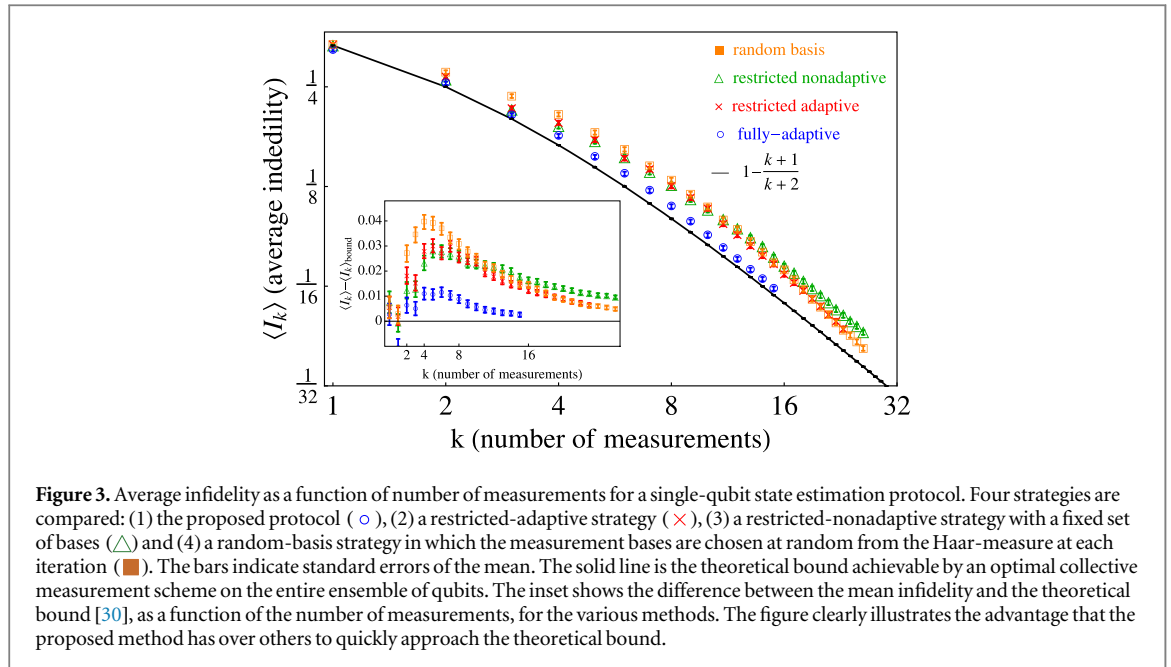


Figure 3. Average infidelity as a function of number of measurements for a single-qubit state estimation protocol. Four strategies are compared: (1) the proposed protocol (\circ), (2) a restricted-adaptive strategy (\times), (3) a restricted-nonadaptive strategy with a fixed set of bases (\triangle) and (4) a random-basis strategy in which the measurement bases are chosen at random from the Haar-measure at each iteration (\blacksquare). The bars indicate standard errors of the mean. The solid line is the theoretical bound achievable by an optimal collective measurement scheme on the entire ensemble of qubits. The inset shows the difference between the mean infidelity and the theoretical bound [30], as a function of the number of measurements, for the various methods. The figure clearly illustrates the advantage that the proposed method has over others to quickly approach the theoretical bound.

direction very close to the most likely state, i.e., the next measurement basis is approximately $\{| \uparrow \rangle, | \downarrow \rangle\}$. This basis differs considerably from the measurement basis obtained by maximizing the fidelity obtained by equation (11).

3.4. Numerical experiments

To test the full capabilities of the strategy proposed here on a qubit system, we conducted $N_{\text{exp}} = 5000$ independent numerical experiments that execute the protocol for a few dozen iterations. In each experiment, a Haar-random pure state $|\Psi\rangle$ was generated to simulate states emitted by the oven, followed by the application of the protocol discussed in section 2. Measurements (one per iteration) were simulated numerically as well, using the generation of random numbers to produce measurement outcomes with the appropriate probabilities, i.e., with probabilities $|\langle e_{k,n} |\Psi\rangle|^2$. Here, k is the measurement (or iteration) index and n labels the basis state. As prescribed by the protocol, the next basis of measurement at every iteration was determined by maximizing the cost function, equation (11), over all possible measurement bases. In the qubit case, since a measurement basis is uniquely defined by a single vector on the Bloch sphere, the optimization here was carried out over the polar and azimuthal angles θ and ϕ . By employing several optimization methods, including exhaustive search, we found conjugate gradient to be the fastest and to yield the most accurate results.

We used the infidelity

$$I_k = 1 - |\langle \Psi | \Psi_k \rangle|^2, \quad (17)$$

as our figure of merit to ascertain the success of our candidate state. For each numerical experiment, we recorded the infidelity I as a function of number of iterations k . Finally, at every iteration k , we averaged the recorded infidelities over the N_{exp} experiments, reporting $\langle I_k \rangle$. (We refer the reader to appendix A for details concerning the actual calculation of the matrices $\varrho_{k,n}$.) The scaling of the average infidelity with the number of iterations, k , determines the performance of the method. The results of our experiments are summarized in figure 3.

Figure 3 shows how our protocol (\circ) compares with three other strategies: a ‘restricted-adaptive’ strategy (\times), a ‘restricted-nonadaptive’ strategy (\triangle), and a ‘random-basis’ strategy where the measurement bases are chosen at random from the Haar-measure (\blacksquare). In the restricted-adaptive strategy the measurements are restricted to the set of Pauli bases, $\{|e_1\rangle\} = \{| \uparrow / \downarrow \rangle\}$, $\{|e_2\rangle\} = \{| \pm \rangle\}$, and $\{|e_3\rangle\} = \{| \pm i \rangle\}$ and the optimization is carried out over this set of bases (see appendix B for more details). In the restricted-nonadaptive strategy, the measurement directions, namely the Pauli x , y and z directions, are simply cycled through repeatedly.

As is clear from the figure, among the four protocols, the optimized protocol gives the best approximation by far to the theoretical bound. This protocol is the solid line in figure 3 and is only achievable by an optimal collective measurement scheme on an ensemble of k qubits $\langle I_k \rangle_{\text{bound}} = 1 - \frac{k+1}{k+2}$ [30]. Additionally, as expected, we find that the restricted-adaptive method performs better than the restricted-nonadaptive strategy and is somewhat comparable to the random basis strategy. The inset to figure 3 shows that the proposed protocol approaches the optimal bound faster than all the other simulated methods.

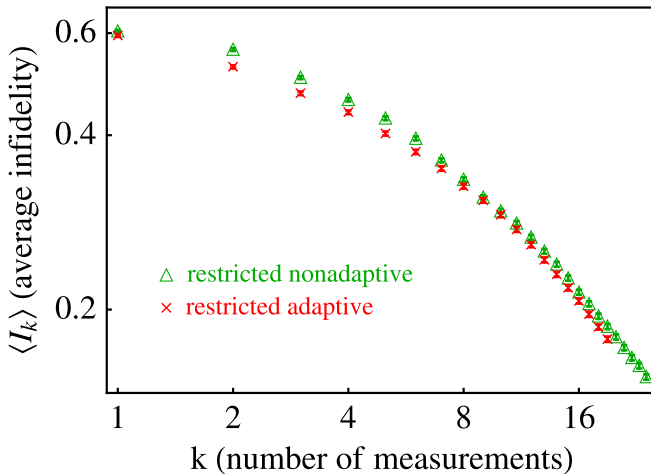


Figure 4. Average infidelity as a function of the number of measurements for a two-qubit state estimation protocol. Two strategies are compared: (1) a restricted-adaptive strategy (\times), and (2) a restricted-nonadaptive strategy (\triangle). The error bars are smaller than the symbols. Even on a restricted set of measurement bases, we find an appreciable advantage in using the adaptive strategy over the nonadaptive one.

4. Optimized two-qubit state estimation with local measurements

To examine the performance of our method in higher dimensions, we consider here the case of two-qubit state estimation. To grant our numerical experiment a more realistic flavor, we assume that the experimenter does not have access to all possible measurement settings, but rather to a small discrete subset of them. Specifically, we consider here a scenario where the experimenter is allowed to measure the qubits only locally in the Pauli bases. Thus, the measurement basis states of the qubits will be of the form $\{|e_n\rangle\} \otimes \{|e_m\rangle\}$, where each qubit set is one of the three bases $\{|\uparrow/\downarrow\rangle\}$, $\{|\pm\rangle\}$ or $\{|\pm i\rangle\}$. In this case, the optimizing protocol, outlined in section 2, can be executed as before, with the obvious modification that the ‘next basis of measurement’ optimization is carried out only over the set of nine available bases. As before, we refer to this procedure as a restricted-adaptive procedure.

Similarly to the procedure described in section 3.4, we conducted $N_{\text{exp}} = 5000$ independent numerical experiments executing the protocol for about a dozen iterations. In each experiment, a Haar-random two-qubit pure state $|\Psi\rangle$ was generated to simulate states emitted by the oven [28]. The local measurements were simulated numerically as well to produce outcomes with the appropriate probabilities, i.e., with probabilities $|\langle e_{n,k} | \langle e_{m,k} | \Psi \rangle|^2$. Here, k is the measurement (or iteration) index and n, m label the basis states of each qubit.

Figure 4 demonstrates how the restricted-adaptive protocol of local Pauli measurements (\times) compares with a nonadaptive strategy in which the available measurement bases are cycled through repeatedly (\triangle). As is clear from the figure, in this scenario too, there is an appreciable gain from the use of the adaptive optimizing protocol.

5. Conclusions and further remarks

We described a fidelity-maximizing, optimized, fully automated quantum state tomography procedure for pure states. The optimality of the protocol is achieved by requiring that each choice of measurement basis results in an estimation that has the highest fidelity to the state representing our knowledge about that emitted by the oven.

We illustrated the power and intuitive interpretation of the proposed technique by considering several theoretical and practical scenarios. Since the protocol described here is optimized at every iteration, no post-processing of the data is required. It would therefore be of particular interest to apply it as an *in situ* procedure in integrated devices for quantum tomography. Such a device would act like a ‘robot,’ correcting itself as needed to find the state emitted by an oven, based on the information it is gathering. In addition, since the protocol is optimal at every stage, it may be stopped at any stage, or after a chosen criterion of confidence or convergence is met. Therefore, no prior knowledge of the number of copies provided by the oven is necessary. In light of the above, we believe that our figure of merit, equation (11), and its generalization to mixed states, could become a useful practical tool for experimentalists to achieve efficient state estimation.

Moreover, we find no obvious reason that the above protocol and formalism could not be straightforwardly generalized to the setting of mixed states or general quantum measurements (POVMs), as well as to cases where prior information about the state-emitting oven is given. We shall consider these generalizations elsewhere.

Finally, we note that an interesting property of the strategy presented here is that it naturally ‘generates’ in its first few iterations, MUBs as bases of measurements; unlike other methods, the protocol does not require *a priori* knowledge of MUBs. Based on this observation, we conjecture that for any d -dimensional system, the first few iterations of our protocol would optimally consist of measuring the system in a sequence of MUBs. For those Hilbert space dimensions for which the number of MUBs is unknown (i.e., if d is not a power of prime [31–34]), this property may be leveraged to answer several outstanding questions associated with the enumeration of MUBs. This avenue of research is currently being pursued by the authors.

Acknowledgments

We thank Gabriel Durkin, Christopher Ferrie and Nathan Wiebe for useful comments and discussions. AK acknowledges support under NSF grant number PHY-1212445. IH acknowledges support under ARO grant number W911NF-12-1-0523. This research used resources of the Oak Ridge Leadership Computing Facility at Oak Ridge National Laboratory, which is supported by the Department of Energy’s Office of Science under Contract DE-AC05-00OR22725.

Appendix A. Calculation of $\varrho_{k,n}$

Following [29], we provide the necessary expressions required for calculating $\varrho_{k,n}$. The basic identity we utilize is

$$\begin{aligned} \langle \phi_k | \cdots \langle \phi_1 | & \left[\int d\psi (|\psi\rangle\langle\psi|)^{\otimes k} \right] |\phi_1\rangle \cdots |\phi_k\rangle \\ &= \frac{(d-1)!}{(k+d-1)!} \text{Per}(\mathcal{M}), \end{aligned} \quad (\text{A1})$$

where $|\psi\rangle$ is an element in a d -dimensional Hilbert space and $\text{Per}(\mathcal{M})$ is the permanent of the $k \times k$ matrix \mathcal{M} whose elements are $\mathcal{M}_{i,j} = \langle \phi_i | \phi_j \rangle$. In our case

$$\varrho_k = \langle \phi_k | \cdots \langle \phi_1 | \left[\int d\psi (|\psi\rangle\langle\psi|)^{\otimes k+1} \right] |\phi_1\rangle \cdots |\phi_k\rangle, \quad (\text{A2})$$

and therefore the matrix elements of ϱ_k in some basis $\{|z_i\rangle\}$ are given by

$$\begin{aligned} \varrho_{k,ij} &\equiv \langle z_i | \varrho_k | z_j \rangle \\ &= \langle z_i | \langle \phi_k | \cdots \langle \phi_1 | \left[\int d\psi (|\psi\rangle\langle\psi|)^{\otimes k+1} \right] |\phi_1\rangle \cdots |\phi_k\rangle | z_j \rangle \\ &= \frac{(d-1)!}{(k+d)!} \text{Per}(\mathcal{A}^{(ij)}), \end{aligned} \quad (\text{A3})$$

where $\mathcal{A}^{(ij)}$ is a $k+1 \times k+1$ matrix that can be written as follows

$$\mathcal{A}^{(ij)} = \begin{pmatrix} \mathcal{M} & V^{(j)} \\ (V^{(i)})^\top & \delta_{i,j} \end{pmatrix}, \quad (\text{A4})$$

and $(V^{(i)})^\top = (\langle e_i | \phi_1 \rangle, \langle e_i | \phi_2 \rangle, \dots, \langle e_i | \phi_k \rangle)$ and similarly for $V^{(j)}$.

Suppose we obtained $k-1$ measurement outcomes. Then, the most likely pure state that describes the system is the state that corresponds to the maximal eigenvalue of ϱ_{k-1} .

To optimize the next measurement basis we first need the eigenvalues of $\varrho_{k,n}$ as a function of the k th measurement outcome, $|\tilde{e}_{k,n}\rangle$, $n = 1, \dots, d$. The matrix elements of $\varrho_{k,n}$ are written (in some computational bases $\{|z_i\rangle\}$) as

$$\begin{aligned} \varrho_{k,n,ij} &\equiv \langle z_i | \varrho_{k,n} | z_j \rangle \\ &= \langle z_i | \langle \tilde{e}_{k,n} | \langle \phi_{k-1} | \cdots \langle \phi_1 | \\ &\quad \times \left[\int d\psi (|\psi\rangle\langle\psi|)^{\otimes k+1} \right] |\phi_1\rangle \cdots |\phi_{k-1}\rangle | \tilde{e}_{k,n} \rangle | z_j \rangle \\ &= \frac{(d-1)!}{(k+d)!} \text{Per}(\mathcal{A}^{(ij)}). \end{aligned} \quad (\text{A5})$$

Appendix B. Single-qubit case: restricted set of measurement bases

In the special case where the set of possible measurement directions is restricted to the x , y and z directions on the Bloch sphere, one does not need to resort to the costly permanents discussed above. In this scenario,

calculations simplify. For example, the product $\prod_{i=1}^k |\langle \hat{n}(\theta_i, \phi_i) | \hat{n}(\theta, \phi) \rangle|^2$ takes the form:

$$\begin{aligned} \prod_{i=1}^k |\langle \hat{n}(\theta_i, \phi_i) | \hat{n}(\theta, \phi) \rangle|^2 &= \frac{1}{2^m} (1 + \cos \theta)^{m_1} (1 - \cos \theta)^{m_2} \\ &\times (1 + \sin \theta \cos \phi)^{m_3} (1 - \sin \theta \cos \phi)^{m_4} (1 + \sin \theta \sin \phi)^{m_5} \\ &\times (1 - \sin \theta \sin \phi)^{m_6}, \end{aligned} \quad (\text{B1})$$

where the m_i denote the number of times the outcomes $| \uparrow \rangle$, $| \downarrow \rangle$, $| + \rangle$, $| - \rangle$, $| +i \rangle$, and $| -i \rangle$ have been obtained, respectively, and $m = \sum_{i=1}^6 m_i$. The above product can be expanded to give:

$$\begin{aligned} &\prod_{i=1}^k |\langle \hat{n}(\theta_i, \phi_i) | \hat{n}(\theta, \phi) \rangle|^2 \\ &= \sum_{k_1, k_2, \dots, k_6=0}^{m_1, m_2, \dots, m_6} \prod_{i=1}^6 \binom{m_i}{k_i} (-1)^{k_2+k_4+k_6} (\cos \theta)^{k_1+k_2} \\ &\times (\sin \theta)^{k_3+k_4+k_5+k_6} (\cos \phi)^{k_4+k_5} (\sin \phi)^{k_5+k_6}. \end{aligned} \quad (\text{B2})$$

In this form, all the integrals (for calculating ϱ_k or $\int dP_k$) will be of the form

$$\int_0^\pi d\theta \cos^m \theta \sin^n \theta = \frac{1 + (-1)^m}{2} \frac{\Gamma\left(\frac{1+m}{2}\right)\Gamma\left(1 + \frac{n-1}{2}\right)}{\Gamma\left(\frac{2+m+n}{2}\right)}, \quad (\text{B3})$$

and

$$\begin{aligned} \int_0^{2\pi} d\phi \cos^m \phi \sin^n \phi &= [1 + (-1)^n] \\ &\times \frac{1 + (-1)^m}{2} \frac{\Gamma\left(\frac{1+m}{2}\right)\Gamma\left(\frac{n+1}{2}\right)}{\Gamma\left(\frac{2+m+n}{2}\right)}. \end{aligned} \quad (\text{B4})$$

Since the integrals are performed explicitly, expressions for obtaining the various matrix entries of ϱ_k and $\int dP_k$ reduce in this case to the more-easily calculable multiple sums over the k_i 's of equation (B2).

References

- [1] Deutsch D and Jozsa R 1992 *Proc. R. Soc. A* **439** 553
- [2] Simon D R 1994 *Proc. 35th IEEE Symp. on Foundations of Computer Science* pp 116–23
- [3] Shor P W 1994 *Proc. 35th IEEE Symp. on Foundations of Computer Science* pp 124–34
- [4] Finilla A B, Gomez M A, Sebenik C and Doll D J 1994 *Chem. Phys. Lett.* **219** 343
- [5] Grover L K 1996 *28th Annual ACM Symp. on the Theory of Computing Proc.* p 212
- [6] Farhi E, Goldstone J, Gutmann S, Lapan J, Ludgren A and Preda D 2001 *Science* **292** 472
- [7] Bennett C H and Brassard G 1984 *Proc. IEEE Int. Conf. on Computers, Systems and Signal Processing* vol 175p 8
- [8] Bennett C and Wiesner S J 1992 *Phys. Rev. Lett.* **69** 2881
- [9] Bennett C H, Brassard G, Crépeau C, Jozsa R, Peres A and Wootters W K 1993 *Phys. Rev. Lett.* **70** 1895
- [10] Bennett C H, Bernstein H J, Popescu S and Schumacher B 1996 *Phys. Rev. A* **53** 2046
- [11] Lloyd S 1997 *Phys. Rev. A* **55** 1613
- [12] Bennett C H, Shor P W, Smolin J A and Thapliyal A V 2002 *IEEE Trans. Inf. Theory* **48** 2637
- [13] Lloyd S 1996 *Science* **73** 1073
- [14] Kim K *et al* 2010 *Nature* **465** 590
- [15] Islam R *et al* 2011 *Nat. Commun.* **2** 377
- [16] Barreiro J T *et al* 2011 *Nature* **470** 486
- [17] Jones K R W 1991 *Ann. Phys.* **207** 140–70
- [18] Jones K R W 1994 *Phys. Rev. A* **50** 3682
- [19] Fischer D G, Kienle S H and Freyberger M 2000 *Phys. Rev. A* **61** 032306
- [20] Hannemann T, Reiss D, Balzer C, Neuhauser W, Toschek P E and Wunderlich C 2002 *Phys. Rev. A* **65** 050303
- [21] Huszár F and Houslsby N M T 2012 *Phys. Rev. A* **85** 052120
- [22] Tanaka F 2012 *Phys. Lett. A* **376** 2471
- [23] Mahler D H, Rozema L A, Darabi A, Ferrie C, Blume-Kohout R and Steinberg A M 2013 *Phys. Rev. Lett.* **111** 183601
- [24] Ferrie C 2014 *Phys. Rev. Lett.* **113** 190404

- [25] Okamoto R, Iefuji M, Oyama S, Yamagata K, Imai H, Fujiwara A and Takeuchi S 2012 *Phys. Rev. Lett.* **109** 130404
- [26] Kravtsov K S, Straupe S S, Radchenko I V, Houlsby N M T, Huszár F and Kulik S P 2013 *Phys. Rev. A* **87** 062122
- [27] Wiebe N, Granade C, Ferrie C and Cory D 2014 *Phys. Rev. A* **89** 042314
- [28] Życzkowski K and Sommers H-J 2001 *J. Phys. A: Math. Gen.* **34** 7111
- [29] Shchesnovich V S 2014 arXiv:[1403.5158](https://arxiv.org/abs/1403.5158)
- [30] Massar S and Popescu S 1995 *Phys. Rev. Lett.* **74** 1259
- [31] Wootters W K and Fields B D 1989 *Ann. Phys., NY* **191** 363
- [32] Bandyopadhyay S, Boykin P O, Roychowdhury V and Vatan F 2002 *Algorithmica* **34** 512
- [33] Klappenecker A and Rötteler M 2004 *Lecture Notes Comp. Sci.* **2948** 262
- [34] Durt T 2005 *J. Phys. A: Math. Gen.* **38** 52671